Spike protein cleavage-activation mediated by the SARS-CoV-2 P681R mutation: a case-study from its first appearance in variant of interest (VOI) A.23.1 identified in Uganda

Laura E. Frazier [1#], Bailey Lubinski [1#], Tiffany Tang [2], Susan Daniel [2], Javier A. Jaimes [3*] and Gary R. Whittaker [3, 4*]

[1] Graduate Program in Biological & Biomedical Sciences, Cornell University, Ithaca, NY, 14853, USA.

[2] Robert Frederick Smith School of Chemical & Biomolecular Engineering, Cornell University, Ithaca, NY, 14853, USA.

[3] Department of Microbiology & Immunology, College of Veterinary Medicine, Cornell University, Ithaca, NY, 14853, USA.

[3] Master of Public Health Program, Cornell University, Ithaca, NY, 14853, USA.

[#] Contributed equally

* Corresponding authors

618 Tower Rd., Ithaca NY 14853, USA

grw7@cornell.edu; jaj246@cornell.edu

Abstract

The African continent is currently notable as a source of novel SARS-CoV-2 variants. The A.23 viral lineage, characterized by three spike mutations F157L, V367F and Q613H, was first identified in a Ugandan prison in July 2020, and then spilled into the general population adding additional spike mutations (R102I, L141F, E484K and P681R) to comprise lineage A.23.1 by September 2020—with this virus being designated a variant of interest (VOI) in Africa and with subsequent spread to 26 other countries. The P681R spike mutation of the A.23.1 VOI is of note as it increases the number of basic residues in the sub-optimal SARS-CoV-2 spike protein furin cleavage site; as such, this mutation may affect viral replication, transmissibility or pathogenic properties. Here, we performed assays using fluorogenic peptides mimicking the S1/S2 sequence from A.23.1 and observed significantly increased cleavability with furin, compared to sequences matching Wuhan-Hu1 S1/S2. We performed functional infectivity assays using pseudotyped MLV particles harboring SARS-CoV-2 spike proteins and observed an increase in transduction for A.23.1-pseudotyped particles in Vero-TMPRSS2 and Calu-3 cells, compared to Wuhan-Hu1, and a lowered infection in Vero E6 cells. However, these changes in infectivity were not reproduced in a P681R point mutant of Wuhan-Hu1 spike. Our findings suggest that while A.23.1 has increased furin-mediated cleavage linked to the P681R mutation—which may affect viral infection and transmissibility—this mutation needs to occur on the background of other spike protein changes to enable its functional consequences.

Introduction

Severe acute respiratory syndrome coronavirus 2 (SARS-CoV-2) is the agent behind the current COVID-19 pandemic (1). SARS-CoV-2 emerged from a yet to be determined animal reservoir and was first identified in late 2019; it has since spread rapidly throughout the world. The virus now exists in two lineages, A and B. While the B lineage became the dominant virus following its introduction into Northern Italy in February 2020, both A and B lineages remain in circulation globally (2). Both lineages have undergone significant diversification as they expanded; with this expansion apparently linked to a key S gene mutation D614G in lineage B and Q613H in lineage A—an apparent example of convergent evolution that resulted in a more stabilized spike protein, with D614G linked to modest increase in virus transmissibility (3). D614G/Q613H have now become established in circulating B/A lineage viruses.

Within the African continent, Uganda has developed an active surveillance system allowing a robust understanding of genomic diversity and molecular epidemiology for SARS-CoV-2 (4, 5). The first COVID case in Uganda was detected in a returning traveler on March 21st 2021, and identified as being caused by an A lineage virus. This first case was rapidly followed by a ban on international passenger flights. However, importation of cases continued via truck drivers arriving from neighboring countries. These cases were mostly caused by B lineage viruses; e.g., B.1.1.1. Within lineage A, the A.23 viral lineage, was first identified in a Ugandan prison in July 2020, and was characterized by three spike mutations F157L, V367F and Q613H (6). This lineage then spilled into the general population adding additional spike mutations (R102I, L141F, E484K and P681R, as well as in nsp6, ORF8 and ORF9—to comprise lineage A.23.1—by September 2020. This virus was subsequently designated a variant of interest (VOI) in Africa, with spread to 26 other countries. By January 2021, A.23.1 comprised over 90% of the viruses sequenced in Uganda (6).

The P681R mutation of A.23.1 is of note as it is part of a proteolytic cleavage site for furin and furin-like proteases at the junction of the spike protein receptor-binding (S1) and fusion (S2) domains (7). The S1/S2 junction of the SARS-CoV-2 S gene has a distinct indel compared to all other SARS-like viruses (sarbecoviruses

in betacoronavirus lineage B)—the amino acid sequence of SARS-CoV-2 S protein is $_{681}$-P-R-R-A-R|S-$_{686}$ with proteolytic cleavage (|) predicted to occur between the arginine and serine residues depicted. Based on nomenclature established for proteolytic events (8), the R|S residues are defined as the P1|P1' residues for enzymatic cleavage, with residue 681 of A.23.1 spike (R681) being the P5 cleavage position. The ubiquitously-expressed serine protease furin is highly specific and cleaves at a distinct multi-basic motif containing paired arginine residues; furin requires a minimal motif of R-x-x-R (P4-x-x-P1), with a preference for an additional basic residue at P2; i.e., R-x-B-R (9). For SARS-CoV-2, the presence of the S1/S2 "furin site" enhances virus transmissibility (10, 11). For A.23.1 S, P681R (P5) provides an additional basic residue and may modulate S1/S2 cleavability by furin, and hence virus infection properties.

We previously studied the role of proteolytic activation of the spike protein of the lineage B SARS-CoV-2 isolates Wuhan-Hu1 and B.1.1.7 (12). Here, we used a similar approach to study the role of the proteolytic activation of the spike protein in the context of the A.23.1 lineage virus, with a focus on the P681R point mutant.

Methods

Furin prediction calculations. ProP: CoV sequences were inputted into the ProP 1.0 Server hosted at: cbs.dtu.dk/services/ProP/. PiTou: CoV sequences were analyzed using the PiTou V3 software hosted at: http://www.nuolan.net/reference.html.

Fluorogenic peptide assays

Fluorogenic peptide assays were performed as described previously with minor modifications (13). Each reaction was performed in a 100 µl volume consisting of buffer, protease, and SARS-CoV-2 S1/S2 WT (TNSPRRARSVA), SARS-CoV-2 S1/S2 B.1.1.7 (TNSHRRARSVA) or SARS-CoV-2 S1/S2 A.23.1 (TNSRRRARSVA) fluorogenic peptide in an opaque 96-well plate. For trypsin catalyzed reactions, 0.8 nM/well TPCK trypsin was diluted in PBS buffer. For furin catalyzed reactions, 1 U/well recombinant furin was diluted

in buffer consisting of 20 mM HEPES, 0.2 mM $CaCl_2$, and 0.2 mM β-mercaptoethanol, at pH 7.5. Fluorescence emission was measured once per minute for 60 continued minutes using a SpectraMax fluorometer (Molecular Devices) at 30°C with an excitation wavelength of 330 nm and an emission wavelength of 390 nm. Vmax was calculated by fitting the linear rise in fluorescence to the equation of a line.

Synthesis and cloning of the A.23.1 spike protein. The sequence for the A.23.1 spike gene from isolate SARS-CoV-2 A.23.1 hCoV-19/Uganda/UG185/2020 (EPI_ISL_955136) was obtained from GISAID, and codon-optimized, synthesized and cloned into a pcDNA 3.1+ vector for expression (GenScript).

Site-directed Mutagenesis

Primers (ACCTGGCTCTCCTTCGGGAGTTTGTCTGG/CCAGACAAACTCCCGAAGGAGAGCCAGGT) for mutagenesis were designed using the Agilent QuickChange Primer Design tool to create the P681R mutation (CCA->CGA). Mutagenesis was carried out on a pcDNA-SARS-CoV-22 Wuhan-Hu 1 S plasmid using the Agilent QuickChange Lightning Mutagenesis kit (The original plasmid was generously provided by David Veesler, University of Washington USA). The mutated pcDNA-SARS-CoV-2 Wuhan-Hu1 P681R S plasmid was used to transform XL-10 gold ultracompetent cells, which were grown up in small culture, and then plasmid was extracted using the Qiagen QIAprep Spin Miniprep Kit. Sanger Sequencing was used to confirm incorporation of the mutation.

Pseudoparticle Generation

Pseudoparticle generation was carried out using a murine leukemia virus (MLV)-based system as previously described with minor modification (14). HEK293T cells were seeded at 2.5x10^5 cells/ml in a 6-well plate the day before transfection. Transfections were performed using polyethylenimine (PEI) and 1X Opti-Mem from Gibco. Cells were transfected with 800 ng of pCMV-MLV-gagpol, 600 ng of pTG-luc, and 600 ng of a plasmid containing the viral envelope protein of choice. Viral envelope plasmids included pcDNA-SARS-CoV-2 Wuhan-Hu1 S as the WT, pcDNA-SARS-CoV-2 Wuhan-Hu1 P681R S, and pcDNA-SARS-CoV-2 A.23.1 S. pCAGGS-VSV G was used as a positive control and pCAGGS was used for a Δ-envelope negative control. At

48 hours post-transfection, the supernatant containing the pseudoparticles was removed, centrifuged to remove cell debris, filtered, and stored at -80°C.

Pseudoparticle Infection Assay

Infection assays were performed as previously described with minor adjustments (14). Vero E6 and Vero-TMPRSS2 cells were seeded at 4.5X10^5 cells/ml in a 24-well plate the day before infection. Calu-3 cells were seeded at 10X10^5 cells/ml in a 24-well plate three days before infection. Cells were washed three times with DPBS and infected with 200 µl of either VSV G, SARS-CoV-2 S, SARS-CoV-2 P681R S, SARS-CoV-2 A.23.1 S, or Δ-envelope pseudoparticles. Infected cells incubated on a rocker for 1.5 hours at 37°C, and then 300 µl of complete media was added and cells were left at 37°C. At 72 hours post-infection, cells were lysed and the level of infection was assessed using the Promega Luciferase Assay System. The manufacturer's protocol was modified by putting the cells through 3 freeze/thaw cycles after the addition of 100 µl of the lysis reagent. 10 µl of the cell lysate was added to 20 µl of luciferin, and then luciferase activity was measured using the Glomax 20/20 luminometer (Promega). Vero E6 and Vero-TMPRSS2 infection assays were replicated four times. The Calu-3 infection assays were replicated three times. Each assay was performed as technical replicates, with the same batch of pseudoparticles used for all of data.

Western blot analysis of pseudoparticles. 3 ml pseudoparticles were pelleted using a TLA-55 rotor with an Optima-MAX-E ultracentrifuge (Beckman Coulter) for 2 hours at 42,000 rpm at 4°C. Particles were resuspended in 26 µl DPBS buffer. Sodium dodecyl sulfate (SDS) loading buffer and DTT were added to samples and heated at 65°C for 20 minutes, making the final volume 40 µl. 30 µl of each sample was separated on NuPAGE Bis-Tris gel (Invitrogen) and transferred on polyvinylidene difluoride membranes (GE). SARS-CoV-2 S was detected using a rabbit polyclonal antibody against the S2 domain (Cat: 40590-T62, Sinobiological) and an AlexaFluor 488 goat anti-rabbit antibody. A mouse monoclonal antibody against MLV p30 (ab130757, Abcam) and an AlexaFluor 488 goat anti-mouse antibody (Invitrogen) were used as a loading control. Bands were detected using the ChemiDoc Imaging software (Bio-Rad).

Results

Bioinformatic and biochemical analysis of the SARS-CoV-2 A.23.1 S1/S2 cleavage site

To gain insight into proteolytic processing at the S1/S2 site of the A.23.1 spike protein, we first took a bioinformatic approach utilizing the PiTou (15) and ProP (16) cleavage prediction tools, comparing A.23.1 to B.1.1.7 and the prototype SARS-CoV-2 Wuhan-Hu1—as well as to SARS-CoV-1, MERS-CoV, and selected other human respiratory betacoronaviruses (HCoV-HKU1 and HCoV-OC43); **Figure 1.** Both algorithms predicted a significant increase in the furin cleavage for A.23.1 compared to Wuhan-Hu1 and B.1.1.7; in comparison SARS-CoV-1 is not predicted to be furin-cleaved; as expected MERS-CoV showed a relatively low furin cleavage score, with HCoV-HKU1 and HCoV-OC43 showing relatively high furin cleavage scores.

Virus	S1/S2 Sequence	Furin Score PiTou	Furin Score ProP
SARS-CoV-2 (A.1/B.1)	672-ASYQTQTNSP**RR**A**R**|SVASQS-691	+9.196	0.626
SARS-CoV-2 (B.1.1.7)	669-ASYQTQTNS**HRR**A**R**|SVASQS-688	+9.907	0.757
SARS-CoV-2 (A.23.1)	669-ASYQTQTNS**RRR**A**R**|SVASQS-688	**+12.209**	**0.704**
MERS-CoV	738-LPDTPSTLTP**R**SV**R**|SVPGEM-757	+5.155	0.563
HCoV-HKU1	747-YNSPSSSSS**RRKRR**|SISASY-766	+14.634	0.918
HCoV-OC43 (clinical)	750-GYCVDYFKN**RR**S**RR**|AITTGY-769	+10.10	0.736

Figure 1. Furin cleavage score analysis of CoV S1/S2 cleavage sites. CoV S sequences were analyzed using the ProP[1] 1.0 and PiTou[2] 3.0 furin prediction algorithm, generating a score with bold numbers indicating predicted furin cleavage. (|) denotes the position of the predicted S1/S2 cleavage site. Basic resides, arginine (R) and lysine (K), are highlighted in blue, with histidine in purple. Sequences corresponding to the S1/S2 region of SARS-CoV-2 (QHD43416.1), SARS-CoV (AAT74874.1), MERS-CoV (AFS88936.1), HCoV-HKU1 (AAT98580.1), HCoV-OC43 (KY369907.1) were obtained from GenBank. Sequences corresponding to the S1/S2 region of SARS-CoV-2 B.1.1.7 (EPI_ISL_1374509) and SARS-CoV-2 A.23.1 hCoV-19/Uganda/UG185/2020 (EPI_ISL_955136), were obtained from GISAID.

To directly address the activity of furin on the SARS-CoV-2 A.23.1 S1/S2 site, we used a biochemical peptide cleavage assay (13). The specific peptide sequences used here were TNSPRRRARSVA (A.23.1 S1/S2) and TNSPRRARSVA (Wuhan-Hu1 S1/S2). We tested furin, along with trypsin as a control **(Figure 2).** As predicted, furin effectively cleaved Wuhan-Hu1 (WT) but with a significant increase for A.23.1 S1/S2. As expected, trypsin also effectively cleaved A.23.1 S1/S2. This comparative data with SARS-CoV S1/S2 sites

reveals that the acquisition of the 618R mutation significantly increase cleavability by furin, with increases beyond that seen for B.1.1.7 (P681) (12).

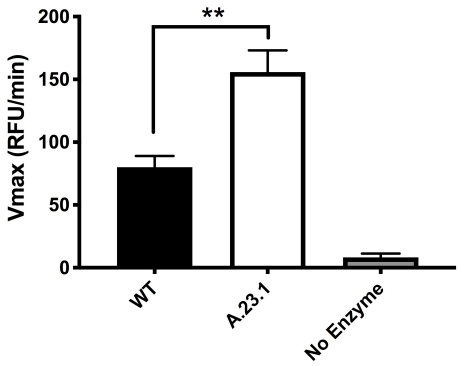

Figure 2. Fluorogenic peptide cleavage assays of the SARS-CoV-2 S1/S2 cleavage site. Peptides mimicking the S1/S2 site of the SARS-CoV-2 Wuhan-Hu1 (WT) and A.23.1 variants were evaluated for *in vitro* cleavage by furin, compared to a control without protease.

Functional analysis of virus entry using viral pseudoparticles

To assess the functional importance of the S1/S2 site for SARS-CoV-2 entry, we utilized pseudoparticles consisting of a murine leukemia virus (MLV) core displaying a heterologous viral envelope protein to recapitulate the entry process of the native counterpart—particles also contain a luciferase reporter that integrates into the host cell genome to drive expression of luciferase, which is quantifiable (14). In this study, MLV pseudoparticles containing the A.23.1, Wuhan-Hu1 SARS-CoV-2 S protein (WT), and a P681R point mutant of Wuhan-Hu1 were also generated alongside positive control particles containing the vesicular stomatitis virus (VSV) G protein, along with negative control particles (Δenvpp) lacking envelope proteins (not shown), using the HEK293T cell line for particle production.

We examined infection of SARS-CoV-2 pseudoparticles in Vero cell lines representative of both the "early" and "late" cell entry pathways **(Figure 3),** as well as cell representative of the human respiratory tract (Calu-3)—as the entry mechanisms of SARS-CoV-2 can be highly cell-type dependent (1). Specifically, we used the Vero-TMPRSS2 and Calu-3 ("early pathway") and the Vero E6 ("late pathway") cell lines, which are predicted to activate the SARS-CoV-2 S2' using TMPRSS2 and cathepsin L respectively. While Vero-TMPRSS2 and Calu-3 cells gave overall significantly higher luciferase signal indicative of more efficient entry, we observed lowered infection in Vero E6 cells. As expected, VSVpp (positive control) infected both cell lines with several orders of magnitude higher luciferase units than the values reported with Δenvpp infection (negative control). We

observed no difference in infection between pseudoparticles displaying spike protein from our P681R point mutant in Calu-3 cells and lowered infection on Vero E6 and Vero-TMPRSS2 cells.

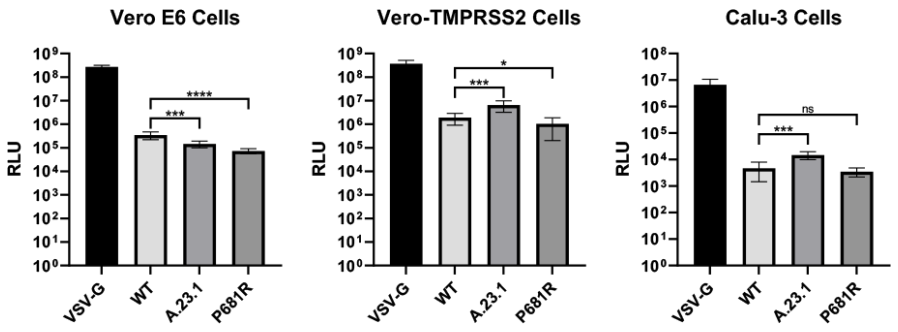

Figure 3. Pseudoparticle infectivity assays in Vero E6, Vero-TMPRSS2 or Calu-3 cells. Cells were infected with MLVpps harboring the VSV-G, SARS-CoV-2 S (WT), SARS-CoV-2 S A.23.1 variant, SARS-CoV-2 S WT with P681R mutation. Data represents the average luciferase activity of cells of three (Vero E6 and Vero-TMPRSS2) or two (Calu-3) biological replicates.

The pseudoparticles were also probed for their S content via western blot and densitometry. For both A.23.1 and Wuhan-Hu1 P681R particles, we detected increased cleavage of the spike protein compared to Wuhan-Hu1 (WT); see **Figure 4.**

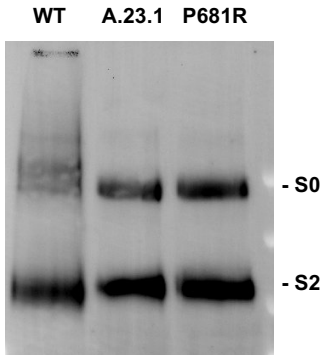

Figure 4. Western blot analysis of SARS-CoV-2 pseudoparticles generated with SARS-CoV-2 Wuhan Hu-1 S (WT), SARS-CoV-2 S A.23.1 variant, or SARS-CoV-2 S WT with P681R mutation. Uncleaved (S0) and cleaved (S2) bands are indicated. SARS-CoV-2 S was detected using a rabbit antibody against the SARS-CoV-2 S2 region. Equivalent MLV content was confirmed using a mouse antibody against MLVp30 (not shown).

Discussion

Since late 2020, the evolution of the SARS-CoV-2 pandemic has been characterized by the emergence of sets of mutations, designated "variants of concern" (VOCs) and "variants of interest" (VOIs). These variants appear to have expanded following the prior introduction of stabilizing mutations into the spike protein, such as D614G and Q613H. The mutations within the VOCs and VOIs impact several virus characteristics including transmissibility and antigenicity, in response to the changing immune profile and social dynamics of the human population (17-21).

To date, the most prevalent SARS-CoV-1 VOC of 2021 has been B.1.1.7. This VOC is characterized by a P681H mutation in the spike S1/S2 "furin cleavage site" and has been linked to increased transmissibility due to the presence of the additional basic amino acid, histidine (H). However, histidine is unusual in that it has an ionizable side chain with a p*K*a near neutrality (22), and so is not conventionally considered a basic amino acid. Most recently, a new VOC B.1.617.2 has replaced B.1.1.7 as the dominant circulating virus globally, which (along with the other sub-lineages B.1.617.1 and B.1.617.3) has a P681R point mutation, and is more conventionally "polybasic" in the S1/S2 cleavage motif and suggested to enhance transmissibility and pathogenesis (23, 24). However, the A.23.1 variant pre-dated B.1.617 as a P681R-containing VOC/VOI by several months. A.23.1 emerged in Uganda beginning in October 2020, to become the dominant virus in the country (89% prevalence on January 12th 2021) **(Figure 5)**. However, during the early months of 2021 other variants also became prevalent in Uganda, including B.1.1.318 and B.1.1.7. During the late spring of 2021, A.23.1 became extinct (1% prevalence on May 5th 2021), with this and other variants being replaced by VOC B.1.351 and VOI B.1.525 (without P681R), and increasingly B.1.617.2—which contains P681R **(Figure 5)**.

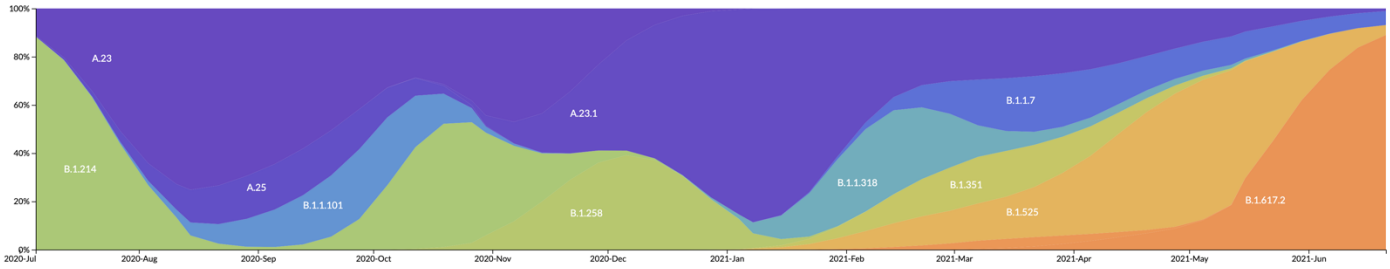

Figure 5. Distribution of SARS-CoV-2 variants in Uganda as assessed by sequencing data (July 2020 – June 2021).
Image was created using Nextstrain.org, according to the following parameters:
https://nextstrain.org/ncov/africa?c=pango_lineage&f_country=Uganda (accessed on June 30th 2021)

Overall, this epidemiological data, suggests that while the P681R point mutation is important for furin-mediated cleavage, it is not the primary driver of virus transmissibility, a finding reinforced by the molecular studies described here.

While P681R does make the S1/S2 cleavage site more basic in nature, such variant cleavage sites are still not "ideal" for furin—as originally found in the prototype furin-cleaved virus mouse hepatitis virus (MHV) (RRARR|S) (25). The introduction of an arginine residue does appear to be making S1/S2 more "polybasic"

as the pandemic continues and transmissibility increases. While we always need to remember not to over-simply the complex process of spike protein activation, it will be interesting to see whether this progression of basic residue addition continues with new variants, towards that seen in established community-acquired respiratory (CAR) coronaviruses such as HCoV-HKU-1 or HCoV-OC43, with S1/S2 sequences of RRKRR|S and RRSRR|A respectively.

Acknowledgements

This work was funded by the National Institute of Health research grant R01AI35270. TT is supported by the National Science Foundation Graduate Research Fellowship Program under Grant No. DGE-1650441 and the Samuel C. Fleming Family Graduate Fellowship. We would especially like to thank Jean Millet, Hector Aguilar-Carreno and Ruth Collins for important insight, and all members of the Daniel and Whittaker groups for helpful discussions.

References

1. Whittaker GR, Daniel S, Millet JK. 2021. Coronavirus entry: how we arrived at SARS-CoV-2. Curr Opin Virol 47:113-120.
2. Rambaut A, Holmes EC, O'Toole A, Hill V, McCrone JT, Ruis C, du Plessis L, Pybus OG. 2020. A dynamic nomenclature proposal for SARS-CoV-2 lineages to assist genomic epidemiology. Nat Microbiol 5:1403-1407.
3. Zhou B, Thao TTN, Hoffmann D, Taddeo A, Ebert N, Labroussaa F, Pohlmann A, King J, Steiner S, Kelly JN, Portmann J, Halwe NJ, Ulrich L, Trueb BS, Fan X, Hoffmann B, Wang L, Thomann L, Lin X, Stalder H, Pozzi B, de Brot S, Jiang N, Cui D, Hossain J, Wilson MM, Keller MW, Stark TJ, Barnes JR, Dijkman R, Jores J, Benarafa C, Wentworth DE, Thiel V, Beer M. 2021. SARS-CoV-2 spike D614G change enhances replication and transmission. Nature 592:122-127.
4. Bugembe DL, Kayiwa J, Phan MVT, Tushabe P, Balinandi S, Dhaala B, Lexow J, Mwebesa H, Aceng J, Kyobe H, Ssemwanga D, Lutwama J, Kaleebu P, Cotten M. 2020. Main Routes of Entry and Genomic Diversity of SARS-CoV-2, Uganda. Emerg Infect Dis 26:2411-2415.
5. Wilkinson E, Giovanetti M, Tegally H, San JE, Lessels R, Cuadros D, Martin DP, Zekri A-RN, Sangare AK, Ouedraogo A-S, Sesay AK, Hammami A, Amuri AA, Sayed A, Rebai A, Elargoubi A, Trotter AJ, Keita AK, Sall AA, Kone A, Souissi A, Gutierrez AV, Page AJ, Iranzadeh A, Lambisia A, Sylverken A, Ibrahimi A, Dhaala B, Kouriba B, Kleinhans B, Brook C, Williamson C, Pratt CB, Akoua-Koffi CG, Agoti CN, Morang'a CM, Nokes DJ, Bridges DJ, Bugembe DL, Baker D, Doolabh D, Ssemwanga D, Tshabuila D, Bassirou D, Amuzu DSY, Goedhals D, Maruapula D, Foster-Nyarko E, Lusamaki EK, Simulundu E, et al. 2021. A year of genomic surveillance reveals how the SARS-CoV-2 pandemic unfolded in Africa. medRxiv doi:10.1101/2021.05.12.21257080:2021.05.12.21257080.
6. Bugembe DL, V.T.Phan M, Ssewanyana I, Semanda P, Nansumba H, Dhaala B, Nabadda S, O'Toole ÁN, Rambaut A, Kaleebu P, Cotten M. 2021. A SARS-CoV-2 lineage A variant (A.23.1) with altered spike has emerged and is dominating the current Uganda epidemic. medRxiv doi:10.1101/2021.02.08.21251393:2021.02.08.21251393.
7. Jaimes JA, Andre NM, Chappie JS, Millet JK, Whittaker GR. 2020. Phylogenetic Analysis and Structural Modeling of SARS-CoV-2 Spike Protein Reveals an Evolutionary Distinct and Proteolytically Sensitive Activation Loop. J Mol Biol 432:3309-3325.
8. Polgár L. 1989. General Aspects of Proteases, p 43-86, Mechanisms of Protease Action. CRC press, Boca Raton, FL.
9. Seidah NG, Prat A. 2012. The biology and therapeutic targeting of the proprotein convertases. Nat Rev Drug Discov 11:367-83.
10. Johnson BA, Xie X, Bailey AL, Kalveram B, Lokugamage KG, Muruato A, Zou J, Zhang X, Juelich T, Smith JK, Zhang L, Bopp N, Schindewolf C, Vu M, Vanderheiden A, Winkler ES, Swetnam D, Plante JA, Aguilar P, Plante KS, Popov V, Lee B, Weaver SC, Suthar MS, Routh AL, Ren P, Ku Z, An Z, Debbink K, Diamond MS, Shi PY, Freiberg AN, Menachery VD. 2021. Loss of furin cleavage site attenuates SARS-CoV-2 pathogenesis. Nature 591:293-299.
11. Peacock TP, Goldhill DH, Zhou J, Baillon L, Frise R, Swann OC, Kugathasan R, Penn R, Brown JC, Sanchez-David RY, Braga L, Williamson MK, Hassard JA, Staller E, Hanley B, Osborn M, Giacca M, Davidson AD, Matthews DA, Barclay WS. 2020. The furin cleavage site of SARS-CoV-2 spike protein is a key determinant for transmission due to enhanced replication in airway cells. bioRxiv doi:10.1101/2020.09.30.318311:2020.09.30.318311.
12. Lubinski B, Tang T, Daniel S, Jaimes JA, Whittaker GR. 2021. Functional evaluation of proteolytic activation for the SARS-CoV-2 variant B.1.1.7: role of the P681H mutation. bioRxiv doi:10.1101/2021.04.06.438731.
13. Jaimes JA, Millet JK, Whittaker GR. 2020. Proteolytic Cleavage of the SARS-CoV-2 Spike Protein and the Role of the Novel S1/S2 Site. iScience 23:101212.
14. Millet JK, Tang T, Nathan L, Jaimes JA, Hsu HL, Daniel S, Whittaker GR. 2019. Production of Pseudotyped Particles to Study Highly Pathogenic Coronaviruses in a Biosafety Level 2 Setting. J Vis Exp doi:10.3791/59010.
15. Tian S, Huajun W, Wu J. 2012. Computational prediction of furin cleavage sites by a hybrid method and understanding mechanism underlying diseases. Sci Rep 2:261.

16. Duckert P, Brunak S, Blom N. 2004. Prediction of proprotein convertase cleavage sites. Protein Eng Des Sel 17:107-12.

17. Muller NF, Wagner C, Frazar CD, Roychoudhury P, Lee J, Moncla LH, Pelle B, Richardson M, Ryke E, Xie H, Shrestha L, Addetia A, Rachleff VM, Lieberman NAP, Huang ML, Gautom R, Melly G, Hiatt B, Dykema P, Adler A, Brandstetter E, Han PD, Fay K, Ilcisin M, Lacombe K, Sibley TR, Truong M, Wolf CR, Boeckh M, Englund JA, Famulare M, Lutz BR, Rieder MJ, Thompson M, Duchin JS, Starita LM, Chu HY, Shendure J, Jerome KR, Lindquist S, Greninger AL, Nickerson DA, Bedford T. 2021. Viral genomes reveal patterns of the SARS-CoV-2 outbreak in Washington State. Sci Transl Med 13.

18. Richard D, Shaw LP, Lanfear R, Acman M, Owen CJ, Tan CC, van Dorp L, Balloux F. 2021. A phylogeny-based metric for estimating changes in transmissibility from recurrent mutations in SARS-CoV-2. bioRxiv doi:10.1101/2021.05.06.442903:2021.05.06.442903.

19. Grubaugh ND, Hodcroft EB, Fauver JR, Phelan AL, Cevik M. 2021. Public health actions to control new SARS-CoV-2 variants. Cell 184:1127-1132.

20. Peacock TP, Penrice-Randal R, Hiscox JA, Barclay WS. 2021. SARS-CoV-2 one year on: evidence for ongoing viral adaptation. J Gen Virol 102.

21. Harvey WT, Carabelli AM, Jackson B, Gupta RK, Thomson EC, Harrison EM, Ludden C, Reeve R, Rambaut A, Consortium C-GU, Peacock SJ, Robertson DL. 2021. SARS-CoV-2 variants, spike mutations and immune escape. Nat Rev Microbiol doi:10.1038/s41579-021-00573-0.

22. Nelson DL, Cox MM. 2000. Lehninger Principles of Biochemistry. Worth Publishers.

23. Peacock TP, Sheppard CM, Brown JC, Goonawardane N, Zhou J, Whiteley M, de Silva TI, Barclay WS. 2021. The SARS-CoV-2 variants associated with infections in India, B.1.617, show enhanced spike cleavage by furin. bioRxiv doi:10.1101/2021.05.28.446163:2021.05.28.446163.

24. Saito A, Nasser H, Uriu K, Kosugi Y, Irie T, Shirakawa K, Sadamasu K, Kimura I, Ito J, Wu J, Ozono S, Tokunaga K, Butlertanaka EP, Tanaka YL, Shimizu R, Shimizu K, Fukuhara T, Kawabata R, Sakaguchi T, Yoshida I, Asakura H, Nagashima M, Yoshimura K, Kazuma Y, Nomura R, Horisawa Y, Takaori-Kondo A, Nakagawa S, Ikeda T, Sato K. 2021. SARS-CoV-2 spike P681R mutation enhances and accelerates viral fusion. bioRxiv doi:10.1101/2021.06.17.448820:2021.06.17.448820.

25. Sturman LS, Ricard CS, Holmes KV. 1985. Proteolytic cleavage of the E2 glycoprotein of murine coronavirus: activation of cell-fusing activity of virions by trypsin and separation of two different 90K cleavage fragments. J Virol 56:904-11.